Modelling reduced excitability in aged CA1 neurons as a calcium-dependent process

Maria Markaki [a], Stelios Orphanoudakis [a] and Panayiota Poirazi [b]

[a] *Department of Computer Science, University of Crete and Institute of Computer Science, Foundation for Research and Technology-Hellas (FORTH), Vassilika Vouton, P.O.Box 1385, GR 711 10 Heraklion, Crete, Greece. Email: mmarkaki@csd.uoc.gr, orphanou@ics.forth.gr*

[b] *Institute of Molecular Biology and Biotechnology, Foundation for Research and Technology-Hellas (FORTH), Vassilika Vouton, P.O.Box 1527, GR 711 10 Heraklion, Crete, Greece. Email: poirazi@imbb.forth.gr*

Abstract

We use a multi-compartmental model of a CA1 pyramidal cell to study changes in hippocampal excitability that result from aging-induced alterations in calcium-dependent membrane mechanisms. The model incorporates N- and L-type calcium channels which are respectively coupled to fast and slow afterhyperpolarization potassium channels. Model parameters are calibrated using physiological data. Computer simulations reproduce the decreased excitability of aged CA1 cells, which results from increased internal calcium accumulation, subsequently larger post-burst slow afterhyperpolarization, and enhanced spike frequency adaptation. We find that aging-induced alterations in CA1 excitability can be explained by simple coupling mechanisms that selectively link specific types of calcium channels to specific calcium-dependent potassium channels.

Key words: calcium-dependent modulation, aging, sAHP, L-type Ca^{2+} channels

1 Introduction

One of the most devastating consequences of normal aging is the accompanying decline in learning and memory capacity. Despite the amount of research work in the field, the underlying molecular mechanisms associated with these deficits remain uncertain. A number of physiological studies have shown that synaptic plasticity in hippocampal CA1 neurons is impaired with aging, due to subtle functional changes related to calcium dysregulation ([7],[19], for a

review see [20]). Specifically, internal Ca^{2+} accumulation in the soma of aged CA1 neurons increases significantly following a train of action potentials [19]. This increase is largely attributed to an enhanced activity of L-type Ca^{2+} channels (LTCs) [18] and/or to a decrease in the free calcium removal rate by various clearance and buffering mechanisms [20].

L-type Ca^{2+} channels display two opposing feedback mechanisms: calcium-dependent facilitation (CDF) and calcium-dependent inactivation (CDI) [23], collectively termed as delayed facilitation. Delayed facilitation exhibits a slow rising time and decay, and is induced by a short train of action potentials or a depolarizing prepulse [2]. Its time course and activation protocol, are remarkably close to that of the sAHP in hippocampal pyramidal neurons [15]. Previous studies suggested that small conductance calcium-activated potassium channels (SK channels) underlie the sAHP [14], and that its slow kinetics result from direct coupling of SK channels with L-type calcium channels [9], [2]. Further support for this coupling comes from two recent studies where the calcium binding protein calmodulin (CaM) was identified as the calcium sensor mediating both the delayed facilitation of LTCs [23], and the Ca^{2+}-dependent gating of SK channels [21]. Moreover, pharmacological studies have shown that facilitation of LTCs by the addition of K8644 agonist increases sAHP and mimics the effects of aging in young-adult neurons [19], while blockade of LTCs greatly reduces sAHP and spike frequency adaptation in aged CA1 cells [10]. In rats, this blockade is sufficient to reverse the age-related alterations in synaptic plasticity of aged –but not young– CA1 cells [11].

According to recent experimental findings [8], [9], [16], a similar coupling scenario might hold for N-type calcium channels (NTCs) and the calcium-activated large conductance potassium channels (BK channels) underlying the fast AHP. NTCS display calcium-dependent inactivation [8] while their activation is nearly coincident with that of BK channels [9]. During repetitive firing, BK channels inactivate rapidly, accounting for the frequency-dependent decline of the fast AHP and subsequent spike broadening [16]. Since intracellular Ca^{2+} concentration is an indicator of the cell's electrical activity [6], a connection between the above conductances seems reasonable.

Although experimental findings suggest a direct connection between the aforementioned calcium-potassium channel types, no modelling work has been done to investigate the effects of such a coupling on the cell's electrical activity. In this work, we modify a previously developed detailed compartmental model of a CA1 pyramidal neuron [12] to include sAHP and fAHP K^+ channels which are coupled to L- and N-type Ca^{2+} channels, respectively. We propose that this coupling can, to a large extent, explain calcium-dependent aging induced alterations in neuronal excitability.

1.1 Theoretical model

The compartmental model used in this work implements the variable time step method of the NEURON simulation environment [4]. The biophysical model, the morphology of which is shown in fig. 1A, is a refinement of a previous model described in [12]. The model consists of 183 compartments and includes a variety of passive and active membrane mechanisms known to be present in CA1 pyramidal cells. We assume a uniform membrane resistance $Rm = 40k\Omega cm^2$, a uniform intracellular resistivity $Ra = 70\Omega cm$, and a specific membrane capacitance of $1.0\mu F cm^{-2}$. The resting membrane potential of the model neuron is $-70mV$. Active mechanisms include two types of Hodgkin-Huxley-type Na^+ currents (somatic and axonic I_{Na}^{sa}, and dendritic I_{Na}^{d}), three voltage-dependent K^+ currents (I_{Kdr}, I_A, I_m), a fast Ca^{2+}- and voltage-dependent K^+ current, I_{fAHP}, a slow Ca^{2+}-dependent K^+ current, I_{sAHP}, a hyperpolarization-activated non-specific cation current (I_h), a low-voltage activated calcium current I_{CaT}, three types of Ca^{2+}- and voltage-dependent calcium currents, I_{CaN}, I_{CaR} and I_{CaL}, and a persistent sodium current I_{Nap}. Channel equations, distributions and densities of I_{Na}, I_{Kdr}, I_A and I_{fAHP} are described in [13]. The remaining mechanisms are adopted from [1], while additional equations and channel densities are detailed in Appendix A. Main changes to earlier model properties related to the present study are described in the following paragraphs.

A simple, exponentially decaying, Ca^{2+} pool is used to measure local submembrane calcium concentration ($[Ca^{2+}]_i$), which modulates calcium-dependent activation and inactivation of L-, N- and R- type calcium channels [8]. The pool accounts for influx from all types of Ca^{2+} channels, taking into consideration calcium efflux from buffering/clearance mechanisms which are not explicitly modelled. These mechanisms are lumped together in a single parameter, i.e. the decay time constant [3]. We chose a small value for this parameter, so that $[Ca^{2+}]_i$ closely follows variations in calcium influx, with a minimal accumulation of Ca^{2+}. An increase in the value of this parameter corresponds to the slower Ca^{2+} removal from the cytosol of aged CA1 cells.

In order to model the coupling of sAHP with LTCs and fAHP with NTCs we use two additional pools selectively linked to Ca^{2+} influx through LTCs and NTCs. The L-type calcium pool ($[L - Ca^{2+}]_i$) modulates sAHP channels, while the N-type calcium pool ($[N - Ca^{2+}]_i$) regulates fAHP channels.

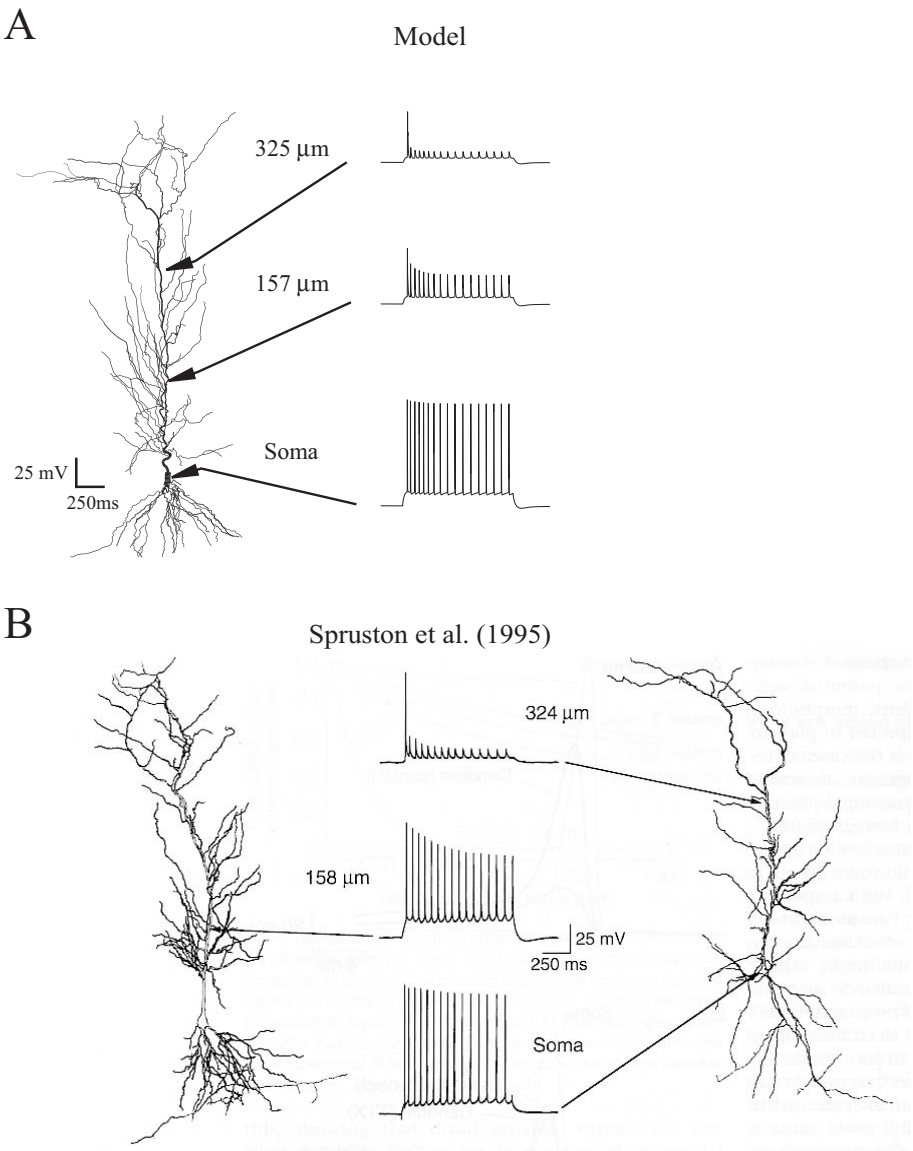

Fig. 1. A. Backpropagating action potentials evoked by somatic current injection (220 pA, 700ms) show typical pattern of distance and time-dependent attenuation of spike height; the attenuation pattern is very similar to experimental traces from Spruston et al (1995) shown in B.

2 Results

2.1 Model Validation

We tested our model cell using a constant depolarizing current injection at the soma while recording simultaneously at the soma and two locations in the apical trunk. We observed a pattern of distance and time-dependent attenuation of back-propagating action potentials (BPAPs) (fig. 1A) similar to that

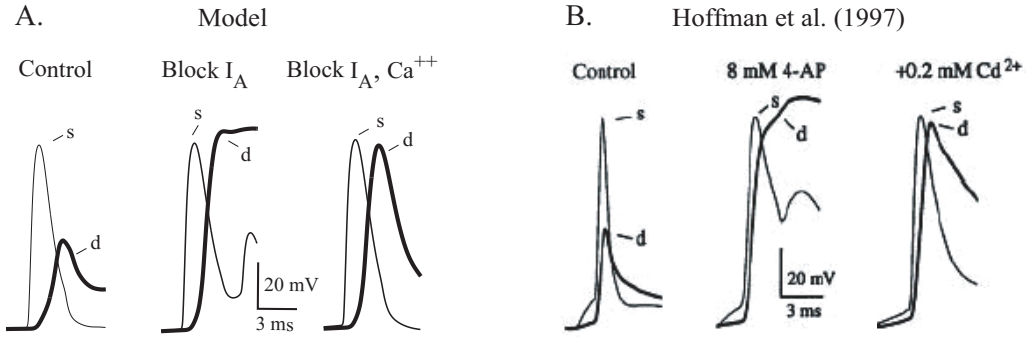

Fig. 2. Initial somatic and dendritic spikes are shown in response to somatic current injection (300 pA, 50 ms) in control conditions (left), with block of I_A (middle) and with block of Ca^{2+} currents (right). Results are comparable to those of Hoffman et al (1997).

reported by [17] (fig. 1B). The only difference is that somatic spikes produced by the model are a few milivolts smaller than experimental traces and this difference in height is propagated in the dendritic traces. Model deviations are more pronounced in middle traces. Note, however, that the respective experimental trace is taken from another cell and may not reflect signal attenuation within a single neuron.

In fig.2A we blocked I_A by 90% throughout the cell, and found that the initial BPAP which under control conditions was severely attenuated at the dendritic recording electrode (fig. 2A, left), reached full height (fig. 2A, middle) as was also observed by [5]. Given the cell is much more excitable in this condition than normal, the dendritic response in both data and model shows a failure to repolarize, as if the voltage were dominated by an unopposed dendritic Ca^{2+} current. When calcium currents were 75% blocked to mimick bath application of 200 mM Cd^{++}, the dendritic spike, though broader than in control conditions, was more fully repolarized (fig. 2A, right). Differences between model and experimental traces include slightly smaller and wider somatic spikes in the model, as well as a stronger repolarization of somatic spikes under both blockade conditions. These differences imply a slightly increased I_A and slightly reduced I_{fAHP} in the model, compared to the experimental cell, which can be improved with further tuning. Overall, model and experimental traces are very similar.

2.2 Effect of aging induced increase in Ca^{2+} influx on electrical activity

To study the effects of aging-induced increase in Ca^{2+} accumulation on the cell's electrical activity, we contrast simulation experiments with electrophysiological recordings from young and aged CA1 pyramidal cells. Figures 3C and 3D show experimental traces from young and aged CA1 cells grouped to

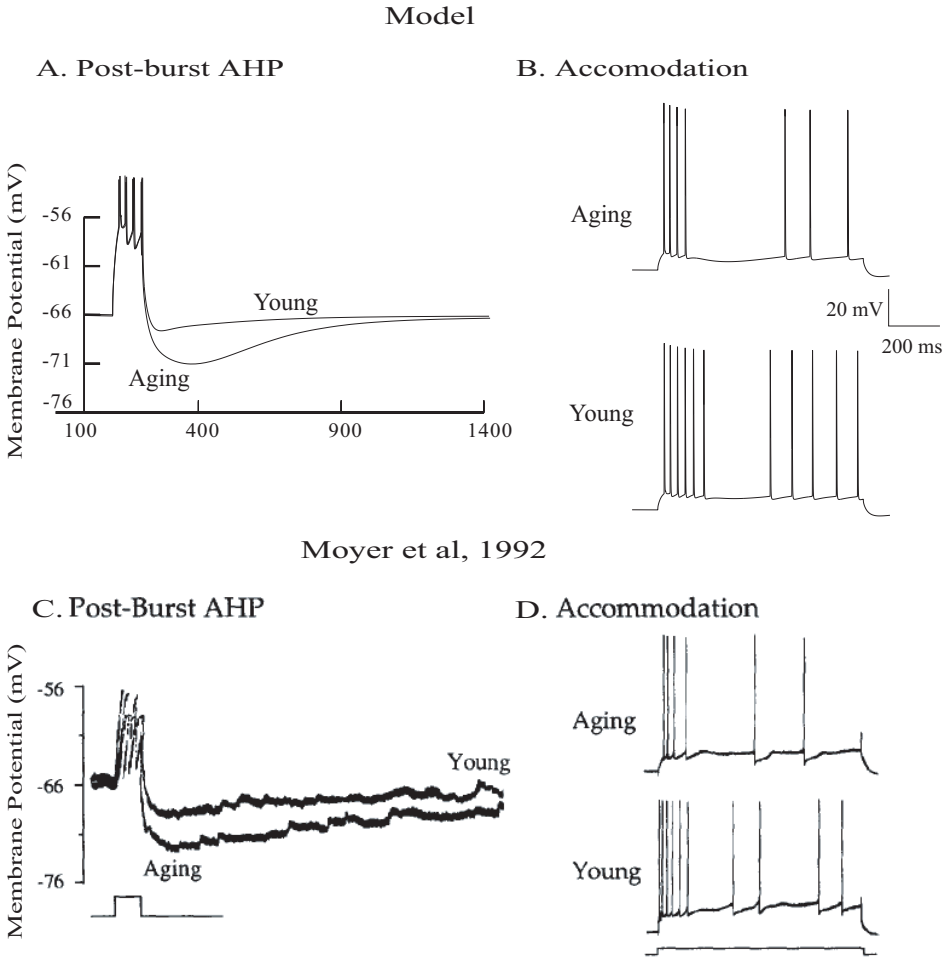

Fig. 3.

Fig. 4. Comparison of model and experimental traces of young vs. old CA1 cells. Model traces are very similar to experimental recordings. A detailed comparison is provided in the text.

equate resting membrane potentials [10]. In fig. 3C, AHP was recorded following a burst of action potentials elicited by a 100-ms depolarizing pulse. The current was adjusted to a minimal level that reliably evoked a burst of four action potentials in both cells. In figure 3D, the same current was injected for 800-ms and the number of action potentials was recorded. Spike frequency adaptation is compared in young vs. aged neurons.

Model simulations are shown in figures 3A and 3B. A rather small increase in the 'young' model's LTC conductance (about 10%) was sufficient to replicate experimental traces for the 'aged' cell. The sAHP and spike frequency adaptation traces were induced using similar to the experimental somatic current injections. Both 'young' and 'aged' model traces are comparable to physiological recordings. Differences in model's sAHP time course and repolarization

potential as well as spike frequency adaptation traces could be eliminated with further refinement of LTC kinetics which drive the slow AHP.

Interestingly, these experimental findings could be reproduced by reducing the decay rate of the global $[Ca^{2+}]_i$ pool model (results not shown). A small increase in the decay time constant - from 2ms to 2.2 ms - resulted in a marked increase in calcium influx from LTCs, presumably because of their positive feedback mechanism (CDF), mimicking the model response produced by increasing LTC conductance.

Fine-tuning of N-type calcium channels and associated fast AHP conductances were not the purpose of this study as these mechanisms are not found to be greatly affected by aging. However, these channels are also affected by calcium influx alterations and their role will be investigated in future work.

3 Conclusions

Using a realistic compartmental model of a CA1 pyramidal neuron, we simulate the cumulative increase of Ca^{2+}-influx observed during aging as a result of (i) a relatively small increase in L-type channel conductance and/or (ii) a small decrease in the decay rate of the intracellular calcium pool, depicting slower calcium removal from the cytosol. We find that both mechanisms cause reduced excitability due to enlarged postburst afterhyperpolarization and enhanced spike-frequency adaptation, similar to that observed in aged CA1 neurons. The model's behavior results from interactions in simple coupling mechanisms which selectively link specific types of calcium channels to specific calcium-dependent potassium channels. Our findings suggest that these coupling mechanisms could serve as the underlying molecular substrate that accounts for aging induced alterations in the cell's electrical activity. Furthermore, competing feedback loops which emerge from these couplings may subserve the fine-tuning of excitability in CA1 neurons. Specifically, due to the delayed facilitation property of LTCs, a train of action potentials in response to a give stimulus would induce a sustained gradual increase in Ca^{2+} influx from these channels that persists during spike intervals. The sAHP current would in turn follow the time course of the L-type calcium signal, causing spike frequency adaptation that eventually ends firing. Since both currents build-up with each spike, they may serve as a record of the recent spiking activity of the cell [6]. If the neuron could in turn use this information to modulate the degree of each channel's contribution, it could tune it's activity to generate different firing patterns in response to different stimuli. Moreover, if aging-induced Ca^{2+} homeostasis dysregulation damages this ability, the cell's information processing capacity would be compensated, resulting in learning and memory deficits.

4 Acknowledgements

This work was partly funded by a Marie Curie Fellowship of the European Community programme Quality of Life under contract number MCF-QLK6-CT-2001-51031, by the Greek GSRT Program ΕΠΑΝ - "Aristeia", code number 1308/B1/3.3.1/317/12.04.2002 and by an ΕΠΕΑΕΚ student fellowship from the University of Crete.

A Model equations

Equations for LTC kinetics are shown below. The time course of delayed facilitation of LTCs is identical to that of sAHP.

$$I_L = g_L * \left(m^2 * h_i([Ca^{2+}]_i) + s_f^2\right) * (v - eca) \tag{A.1}$$

$$h_i([Ca^{2+}]_i) = \frac{k_i}{[Ca^{2+}]_i + k_i} \tag{A.2}$$

$$s_{f_{inf}} = \frac{([Ca^{2+}]_i)^2}{([Ca^{2+}]_i)^2 + b^2} \tag{A.3}$$

$$t_f = t_o + \frac{1}{([Ca^{2+}]_i)^2 + b^2} \tag{A.4}$$

where $t_o = 100ms$, $k_i = 0.025mM$, $b = 0.01mM$ and the somatic conductance value is: $g_L = 0.3mS/cm^2$. The state variable m is described in [1].

The current equation for N-type (and R-type) Ca^{2+} channels is given by:

$$I_N = g_N * m^2 * h * h_i([Ca^{2+}]_i) * (v - eca) \tag{A.5}$$

where the function $h_i()$ is the same as in LTCs and the somatic conductance value is: $g_N = 0.2mS/cm^2$. The state variables m and h are described in [1]

Equations for sAHP channel are given by:

$$I_{sAHP} = g_{sAHP} * m^2 * (v - ek) \tag{A.6}$$

$$m_{inf} = \frac{[L - Ca^{2+}]_i}{[L - Ca^{2+}]_i + b} \tag{A.7}$$

$$t_{inf} = t_o + \frac{1}{[L - Ca^{2+}]_i + b} \tag{A.8}$$

where $t_o = 100ms$, $b = 0.005mM$ and the somatic conductance value is: $g_{sAHP} = 0.025S/cm^2$

References

[1] Borg-Graham L (1998). Interpretations of data and mechanisms for hippocampal pyramidal cell models. In *Cerebral Cortex*, vol 13, *Cortical Models*, ed. JONES EG, ULINSKY PS & PETERS A, 19–138. Kluwer Academic/Plenum Publishers, New York.

[2] Cloues RK, Tavalin SJ, Marrion NV (1997). B-adrenergic stimulation selectively inhibits long-lasting L-type calcium channel facilitation in hippocampal pyramidal neurons. J Neurosci, 17(17):6493–6503.

[3] De Schutter E, Smolen P (1998). Calcium dynamics in large neuronal models. In *Methods in neuronal modeling: From ions to networks*, ed. C. Koch and I. Segev, pp. 211–250. Cambridge: MIT Press.

[4] Hines ML, Carnevale NT (1997). The NEURON simulation environment. Neural computation, 9:1179–1209.

[5] Hoffman DA, Magee JC, Colbert CM, Johnston D (1997). K^+ channel regulation of signal propagation in dendrites of hippocampal pyramidal neurons. Nature, 387:869–875.

[6] Koch C (1999). *Biophysics of computation: Information processing in single neurons*. Oxford University Press.

[7] Landfield
PW, Pitler TA (1984). Prolonged Ca^{2+}-dependent afterhyperpolarizations in hippocampal neurons of aged rats. Science 226:1089–1092.

[8] Liang H, DeMaria CD, Erickson MG, Mori MX, Alseikhan BA, Yue DT (2003). Unified mechanisms of Ca^{2+} regulation across the Ca^{2+} channel family. Neuron, 39:951–960.

[9] Marrion NV, Tavalin SJ (1998). Selective activation of Ca^{2+}-activated K^+ channels by co-localized Ca^{2+} channels in hippocampal neurons. Nature, 395:900-905.

[10] Moyer JR, Thompson LT, Black JP, Disterhoft JF (1992). Nimodipine increases excitability of rabbit CA1 pyramidal neurons in an age- and concentration-dependent manner. J. Neurophysiol, 68:2100–2109.

[11] Norris CM, Halpain S, Foster TC (1998). Reversal of age-related alterations in synaptic plasticity by blockade of L-type Ca^{2+} channels. J Neurosci, 16:5382–5392.

[12] Poirazi P, Brannon T, Mel BW (2003). Arithmetic of Subthreshold Synaptic Summation in a Model CA1 Pyramidal Cell. Neuron, 37:977–987.

[13] Poirazi P, Brannon T, Mel BW (2003). Online Supplement: About the Model. Neuron, 37:977–987.

[14] Sah P (1996). Ca^{2+}-activated K^+ currents in neurons: types, physiological roles and modulation. Trends Neurosci 19:150–154.

[15] Sah P, Clements JD (1999). Photolytic manipulation of $[Ca^{2+}]_i$ reveals slow kinetics of potassium channels underlying the afterhyperpolarization in hippocampal pyramidal neurons. J Neurosci, 19(10):3657–3664

[16] Shao LR, Halvorsrud, Borg-Graham L, Storm JF (1999). The role of BK-type Ca2+-dependent K^+ channels in spike broadening during repetitive firing in rat hippocampal pyramidal cells. J. Physiology 521.1:135–146.

[17] Spruston N, Schiller Y, Stuart G, Sakmann B (1995). Activity-dependent action potential invasion and calcium influx into hippocampal CA1 dendrites. Science, 286:297–300.

[18] Thibault O, Landfield PW (1996). Increase in single L-type calcium channels in hippocampal neurons during aging. Science, 272:1017–1020.

[19] Thibault O, Hadley R, Landfield PW (2001). Elevated postsynaptic $[Ca^{2+}]_i$ and L-type calcium channel activity in aged hippocampal neurons: relationship to impaired synaptic plasticity. J Neurosci, 21(24):9744–9756.

[20] Verkhratsky A, Toescu EC (1998). Calcium and neuronal aging. Trends Neurosci 2:12–17.

[21] Xia XM, Fakler B, Rivard A, Wayman G, Johnson-Pais T, Keen JE, Ishii T, Hirchberg B, Bond CT, Lutsenko S, Maylie J, Adelman JP (1998). Mechanism of calcium gating in small-conductance calcium-activated potassium channels. Nature, 395:503–507.

[22] Yamada WM, Koch C, Adams PR (1998). Multiple channels and calcium dynamics. In *Methods in neuronal modeling: From ions to networks*, ed. C. Koch and I. Segev, pp. 211–250. Cambridge: MIT Press.

[23] Zuhlke RD, Pitt GS, Deisseroth K, Tsien RW, Reuter H (1999). Calmodulin supports both inactivation and facilitation of L-type calcium channels. Nature, 399:159–162.